



Antiwear Properties of Binary Ashless Blend of Phosphonium Ionic Liquids and Borate Esters in Partially Formulated Oil (No Zn)

Vibhu Sharma¹ · Nicole Dörr² · Ali Erdemir³ · Pranesh B. Aswath¹

Received: 17 October 2018 / Accepted: 19 February 2019
© Springer Science+Business Media, LLC, part of Springer Nature 2019

Abstract

In this study, interaction of ionic liquid (IL) and borate esters (SBs) as antiwear (AW) additives with steel surfaces in tribological contacts was examined using blends which contained no prior AW additives but all the other ingredients present in a fully formulated engine oil. In detail, low phosphorus oil blends were prepared by adding trihexyltetradecylphosphonium bis(2-ethylhexyl)phosphate (P_DEHP) at 700 ppm phosphorus and 2-methoxy-4,4,6-trimethyl-1,3,2-dioxaborinane or trimethoxyboroxine at 200 ppm boron treat rate to a partially formulated oil. The tribological properties of these novel ionic liquid (IL) additive and IL + SB additive mixtures were compared with those of zinc dialkyldithiophosphate (ZDDP) at equal phosphorus levels in the oil blends. Tribological experiments with a reciprocating cylinder on flat contact revealed that both P_DEHP and binary mixtures of P_DEHP + SB offer superior wear protection than ZDDP and the partially formulated oil without AW additives, expressed by a wear reduction of minimum 50%. X-ray absorption near edge structure spectroscopy (XANES) analysis revealed that tribologically formed films are primarily composed of calcium phosphate for oils with AW additives. The interaction of P_DEHP with SB results in additional boron oxide/boric acid and to some extent boron phosphate domains incorporated into the tribofilms.

Keywords Ionic liquids · Wear · Borate esters · XANES · Fully formulated oils

1 Introduction

Over the last decade, ionic liquids (ILs) have emerged as a potential antiwear (AW) additive replacement for zinc dialkyldithiophosphate (ZDDP). ILs are regarded as ashless “environmentally friendly” lubricant additives with excellent tribological properties. Thereby, both cation and anion are composed of organic moieties, typically alkyl side chains with different lengths and branching. Besides their high thermo-oxidative stability, low volatility, low flammability, ILs have also shown to possess good antiwear and anti-friction properties [1–18].

ILs based on tetraalkylphosphonium dialkylphosphate have been recently discovered as the most promising ionic

liquid additives for AW applications [4, 8, 10, 19–21]. Barnhill et al. [4] studied the impact of structural modification of the phosphonium cation in the ILs on their tribological properties by designing various alkyl groups (short chain and long chain, symmetric and asymmetric) while keeping the anion structure identical. They reported that larger cation size results in better lubrication properties that go along with improved miscibility in non-polar base oil with critical minimum alkyl chain length of six carbon atoms. Somers et al. [2] confirmed that phosphonium ILs with long alkyl chains on both anion and cation show better miscibility in non-polar base oils. Qu et al. [10] studied the tribological properties of phosphonium phosphate IL and reported comparable or even superior antiwear and anti-scuffing properties than ZDDP in base oil blends.

Interaction of phosphonium phosphate ILs with other AW additives have also been studied. For example, Qu et al. [22] reported that synergistic effects between phosphonium phosphate ILs and ZDDP results in a 30% reduction of friction and more than 70% reduction in wear. In this context, our previous study [19] performed in group 1 mineral base oil, examined the interaction between

✉ Pranesh B. Aswath
Aswath@uta.edu

¹ Materials Science and Engineering Department, University of Texas at Arlington, Arlington, TX, USA

² AC2T research GmbH, Wiener Neustadt, Austria

³ Argonne National Laboratory, Argonne, IL, USA

trihexyltetradecylphosphonium bis(2-ethylhexyl)phosphate (P_DEHP) IL and soluble borate esters (SBs). Aswath et al. [23] found that addition of SBs to P_DEHP in base oil significantly reduces the incubation time for tribofilm formation which consequently results in superior wear protection than ZDDP at equal phosphorus treat rate (i.e., 0.1 wt% phosphorus). X-ray absorption near edge structure spectroscopy (XANES) has the unique capability to investigate the local coordination of elements present on the surface (5–50 nm) and in the bulk of the sample (up to several 100 nm). Chemical analysis of the tribofilms using XANES revealed that exceptional antiwear properties of P_DEHP + SB blends are a result of the formation of BPO_4 together with $FePO_4$ and B_2O_3/H_3BO_3 tribofilms.

In this study, antiwear properties of blends of P_DEHP IL and borate esters (SB) were evaluated in a partially formulated oil (PFO) that did not contain any AW additives (no zinc, no phosphorus). Low phosphorus oil blends were prepared by blending the P_DEHP in partially formulated oil at 700 ppm phosphorus treat rate. Borate ester was blended at 200 ppm boron treat rate. This way, all interactions between the diversity of additives occurring in engine oils could be assessed. Antiwear performance of the now fully formulated engine oils obtained has been determined using a reciprocating cylinder on flat contact operated under pure sliding. Friction and wear properties were compared with those of a reference oil which contained ZDDP at a 700 ppm phosphorus level. Surface topography and 3D profiling of the rubbed surfaces were analyzed using scanning electron microscopy (SEM) and scanning probe microscopy (SPM), respectively. XANES was used to describe the chemical nature of the tribofilms.

2 Experimental Details

2.1 Description of Additive and Oil Chemistries

Table 1 provides details of the additive chemistries used. ZDDP selected in this research work, is a secondary alcohol derived ZDDP with approximately 70% neutral and 30% basic characteristics, details of which are available in Parekh et al. [24]. IL trihexyltetradecylphosphonium bis(2-ethylhexyl)phosphate (P_DEHP) and borate ester 2-methoxy-4,4,6-trimethyl-1,3,2-dioxaborinane (SB1) were provided from AC2T research GmbH, Austria. Trimethoxyboroxine (SB2) was provided by Argonne National Laboratory, USA.

Oil blends were prepared with a partially formulated oil (PFO) based on GF-5 engine oil specification that contained all additives (detergents, dispersants, antioxidants, viscosity index improvers, corrosion inhibitors, etc.) but no AW additives, thus neither zinc (Zn) nor phosphorus (P) as expected

in ZDDP. This partially formulated oil was characterized by a viscosity of 42 mm²/s at 40 °C and 7.7 mm²/s at 100 °C and a viscosity index of 156. Base reserve amounted to a total base number of 7 mg KOH/g oil, which refers to a calcium (Ca) content of about 2000 ppm.

Oil samples for tribological experiments were formulated by blending ZDDP, IL and borate esters individually or as mixtures of IL and SB1 or IL and SB2 in the partially formulated oil. All blends were prepared by keeping the P and boron (B) concentration at 700 ppm and 200 ppm, respectively.

2.2 Tribological Experimental Details

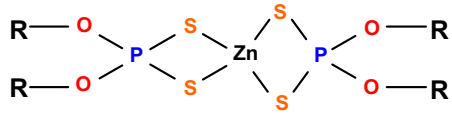
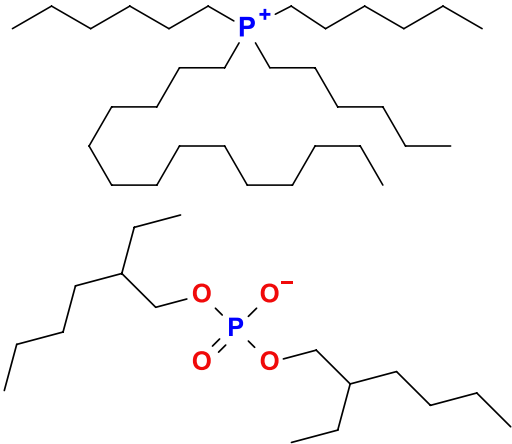
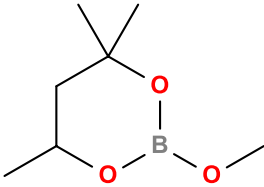
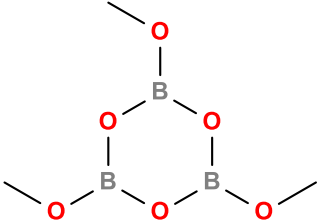
Tribological experiments were conducted at Argonne National Laboratory, Applied Materials Division. Tribological experiments were performed using a cylinder on reciprocating flat contact testing machine [25]. Table 2 provides the schematic of the contact configuration and highlights the tribometrical parameters. Specimens were cleaned before each experiment using Stoddard solution followed by isopropanol and acetone to completely remove any oil and dust present on the surfaces. The rubbed surfaces after the experiments were cleaned with n-heptane and isopropanol and then saved by submerging them in sulfur free base oil.

2.3 Characterization of Tribofilms

Wear scar width generated on the cylinder after rubbing was measured using optical images obtained from an Olympus metallographic microscope. Wear width was measured at nine locations on each cylinder and each oil sample was examined twice. Thus, wear width for each oil sample is an average of 18 measurements. The surface topography of the wear track and wear mechanism was examined by obtaining secondary emission scanning electron microscopy (SEM) images and three-dimensional (3D) images of the rubbed surfaces using Hysitron Triboscope™ in scanning probe microscopy (SPM) imaging mode.

XANES analysis has been used extensively in tribology to examine the chemical composition of the tribofilms [1, 19, 26–37]. Thus in this work, chemical nature of the tribofilms formed during tribological evaluation was also characterized using XANES. XANES spectra were obtained at The Canadian Light Source synchrotron facility at Saskatoon Canada. The phosphorus L-edge (P L-edge) and boron K edge (B K-edge) spectra were collected at variable line spacing plane grating monochromator (VLS-PGM) beam station that operates at the energy range of 5.5–250 eV with a photon resolution of more than 10,000 $E/\Delta E$. All the spectra were collected using a 100 μm x 100 μm photon beam spot size. The phosphorus K-edge, sulfur K-edge and calcium K-edge spectra were obtained from soft X-ray micro characterization

Table 1 Description of additive chemistries

Coded name	Chemical name	Chemical structure
ZDDP	Zinc dialkyldithiophosphate	 <p style="text-align: center;">R = alkyl or aryl group</p>
P_DEHP	Trihexyltetradecylphosphonium bis(2-ethylhexyl) phosphate	
SB 1	2-Methoxy-4,4,6-trimethyl-1,3,2-dioxaborinane	
SB 2	Trimethoxyboroxine	

beam (SXRMB) line which operates at high energy ranging from 1.7 to 10 keV with a photon resolution of 3.3×10^{-4} Insb (111). A $1 \text{ mm} \times 2 \text{ mm}$ spot size was chosen to collect the spectra at the SXRMB line. In this study, XANES spectra were acquired in both total electron yield (TEY) and fluorescent yield (FY) signal detection mode. TEY spectra offer more surface-sensitive information, whereas FY spectra provide information from the bulk of the sample. Typically, in the case of Si L-edge the sampling depth in TEY and FY mode is about 5 nm and 70 nm, respectively [23]. High flux of high-energy soft/hard X-ray photons from a synchrotron radiation source is used to excite core level electrons of an atom. As a result, a vacancy (hole) is created in either K or L levels which subsequently is filled with an electron from higher energy shells followed by emission of a fluorescent photon which is detected by the fluorescence detector inside

the main chamber and plotted as FY spectra. TEY spectra, which provide near surface information, are collected by measuring a neutralization current that is applied to the sample to balance the positive charge created on the sample as X-ray photon absorption leads to the excitation of core level electrons to continuum.

3 Results and Discussion

3.1 Coefficient of Friction and Wear Volume

The coefficients of friction (CoF) obtained from different oil blends are plotted in Fig. 1. The partially formulated oil without AW additive and its blends with AW additives, i.e., P_DEHP, P_DEHP + SB1 and P_DEHP + SB2,

Table 2 Schematic of the contact configuration and details about tribometrical parameters

Tribological test	Reciprocating cylinder on flat contact	
	Front view	Side view
Oil matrix	Partially formulated oil (PFO contained no Zn, no P, but all the other components of a GF-5 oil)	
Oil viscosity	7.7 mm ² /s at 100 °C	
Treat rate	Phosphorus: 700 ppm and boron: 200 ppm	
Applied load	82 N	
Initial Hertzian contact pressure	500 MPa	
Temperature	100 °C	
Speed	Average 0.06 m/s at a frequency of 5 Hz	
Stroke length	6 mm	
Duration	1 h	
Cylinder	Φ 4 mm × 6 mm, 52100 steel, 60–61 HRc	
Flat	12 mm × 12 mm × 8 mm, 52100 steel, 60–61 HRc	

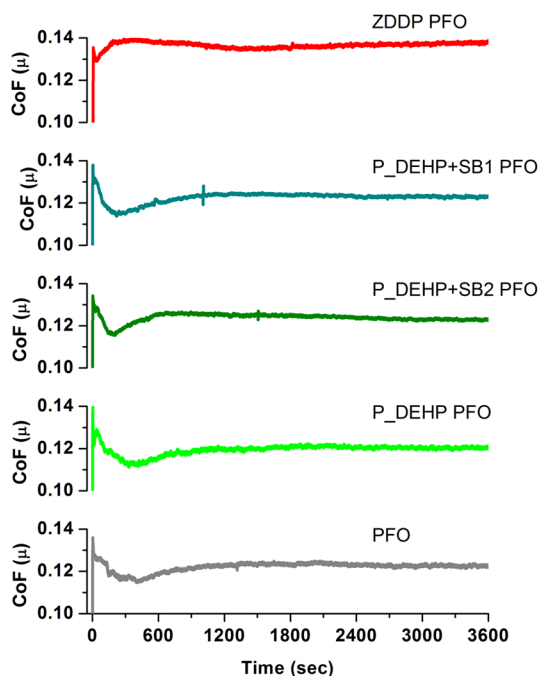


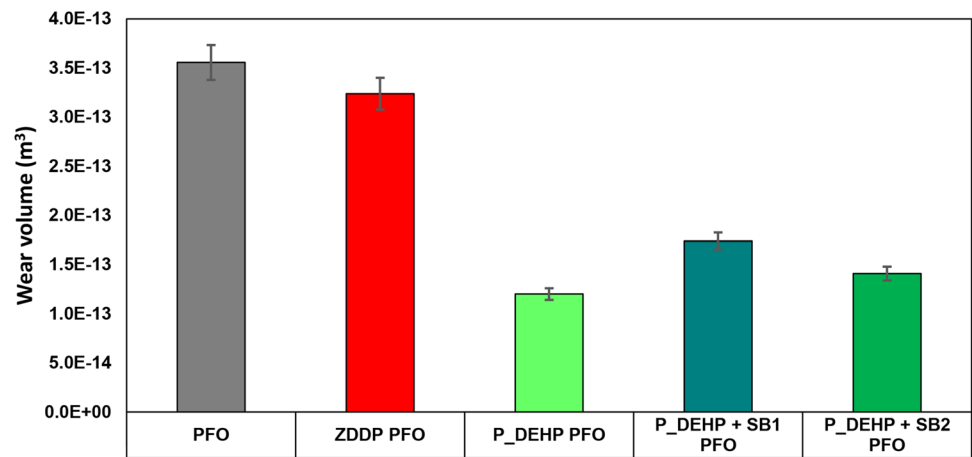
Fig. 1 Coefficient of friction (CoF) as a function of test duration obtained for the partially formulated oil (PFO contained no Zn, no P, but all the other components of a GF-5 oil) and its blends with AW additives (ZDDP, P_DEHP, P_DEHP + SB1 and P_DEHP + SB2)

exhibit similar frictional response as a function of rubbing time. CoF decreases in the initial stages of the tribological experiments (up to ~300 s), then slightly increases (~300–900 s), and eventually remains consistent

(CoF ~0.12) for the rest of the test duration. On the other hand, ZDDP oil blend shows an increase in the CoF in the initial state (up to ~300 s) and then is constant (CoF ~0.14) for the remaining duration. These results indicate that IL and borate ester AW chemistries do not contribute to friction behavior that is different from that of the partially formulated oil. However, the addition of ZDDP to partially formulated oil leads to an increase in the CoF value. All friction curves are characterized by a smooth progress, hence do not indicate the presence of severe adhesion due to direct metal–metal contacts.

The antiwear performance of P_DEHP and binary additive mixtures of P_DEHP with SB1 or SB2 in PFO was benchmarked against that of partially formulated oil without AW and with ZDDP. Wear volumes determined on the cylinder specimens are shown in Fig. 2. The error bars denote the standard deviations calculated from 18 individual measurements each. Partially formulated oil exhibited the highest wear volume whereas the addition of AW additives resulted in wear volume reduction. In detail, ZDDP could only slightly reduce wear. Statistically, wear by ZDDP in PFO (wear reduction of 9%) is in the range of wear by PFO when used alone. On the other hand, antiwear performance of PFO blended with P_DEHP as well as with binary mixtures of P_DEHP + SB1 and P_DEHP + SB2 was significantly improved. Oil blends with P_DEHP resulted in the lowest wear volume (wear reduction of 66%) followed by P_DEHP + SB2 (wear reduction of 60%) and P_DEHP + SB1 (wear reduction of 51%).

Fig. 2 Wear volumes measured for the partially formulated oil (PFO) and its blends with AW additives (ZDDP, P_DEHP, P_DEHP+SB1 and P_DEHP+SB2)

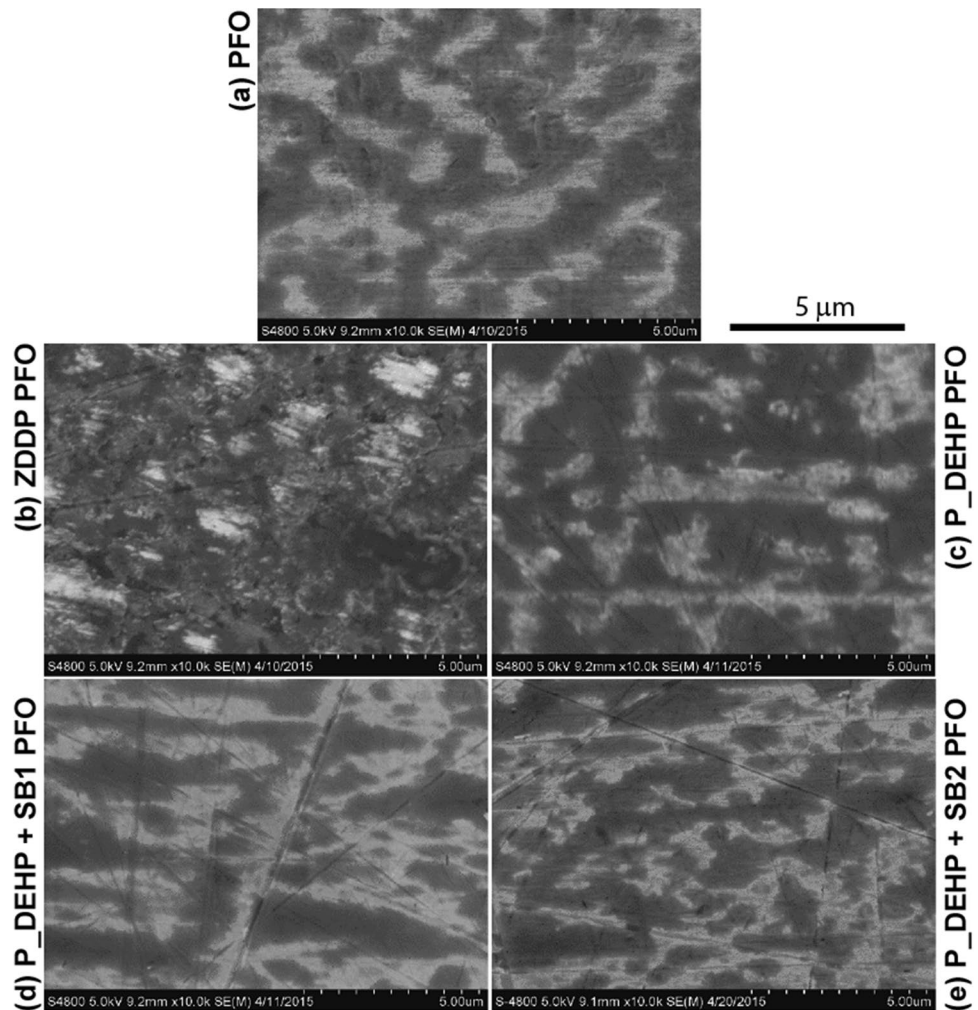


3.2 Wear Scars Characterized by SEM and SPM

Tribofilms and topographical features derived on the mating surfaces after rubbing were examined using SEM and SPM imaging techniques. SEM images of the wear tracks

generated on the flat specimens are presented in Fig. 3. Wear surfaces typically exhibit three features, i.e., bright region, darker region and region of material removal such as scratches and metal pull-out. Bright regions were generated by mainly metallic surfaces (Fe surfaces) whereas darker

Fig. 3 SEM images of the wear tracks generated on the flat specimens with **a** PFO, **b** ZDDP in PFO, **c** P_DEHP in PFO, **d** P_DEHP + SB1 in PFO and **e** P_DEHP + SB2 in PFO



regions can be attributed to higher abundances of light elements that originate from the oil blends (tribofilms). Flat specimen lubricated with PFO (Fig. 3a) exhibited a uniform distribution of banded bright and dark areas, suggesting that wear surfaces are covered with tribofilms to some extent. In addition, regions of metal pull-out are also evident, indicating abrasive-type wear conditions. ZDDP in PFO (Fig. 3b) derived wear surfaces that showed a few mild scratches in addition to the bright and dark areas with a larger coverage of tribofilms (dark areas) than PFO without AW additives. Similarly, oil blends with P_DEHP (Fig. 3c), P_DEHP + SB1 (Fig. 3d) and P_DEHP + SB2 (Fig. 3e) have generated wear surfaces with a few mild scratches together with regions of tribofilm coverage characterized by dark areas of varying shape and size. The comparison with ZDDP shows that oil

blends with P_DEHP exhibited larger patches of tribofilms with higher contrast that suggests thicker tribofilms.

Figure 4 shows the 3D profiles of the wear tracks found on the flat specimen after rubbing acquired by SPM imaging. The arrow next to the image Fig. 4a denotes the sliding direction. SPM images were produced for $60\ \mu\text{m} \times 60\ \mu\text{m}$ areas while keeping the z-axis same, i.e., $\pm 200\ \text{nm}$. Tribofilms from PFO (Fig. 4a) exhibited small pad-like features across the wear track. SPM image of tribofilms from ZDDP in PFO (Fig. 4b) revealed island-type features that are typical of ZDDP tribofilms [25, 38]. These features were more pronounced with ZDDP in PFO than with PFO when used alone. In the case of oil blends with P_DEHP (Fig. 4c), surface topography was similar to PFO. Wear track was consistently covered with a tribofilm composed of island-type

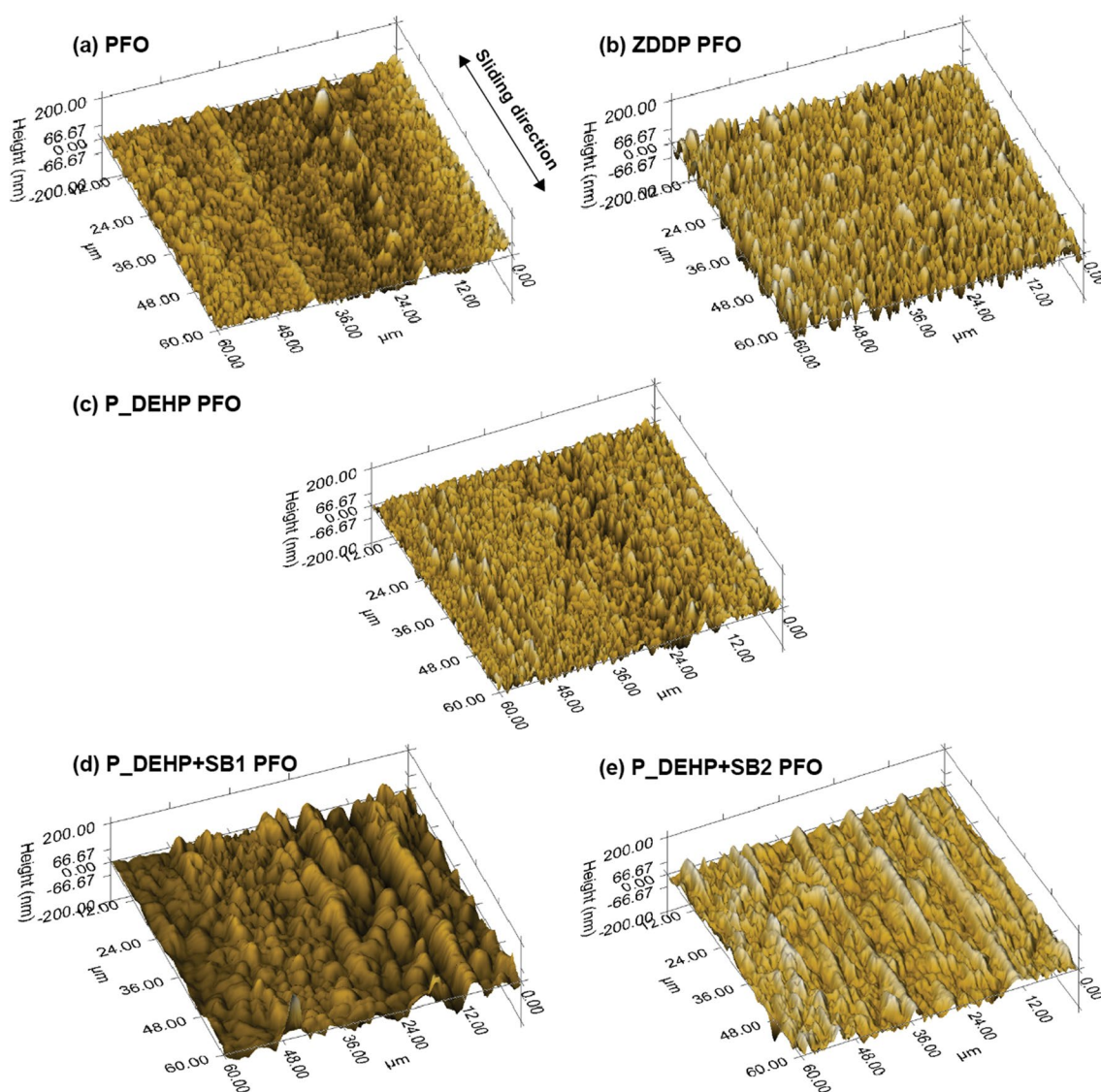


Fig. 4 SPM images of the wear tracks generated on the flat specimens with **a** PFO, **b** ZDDP in PFO, **c** P_DEHP in PFO, **d** P_DEHP+SB1 in PFO and **e** P_DEHP+SB2 in PFO

patches. Oil blends that contained P_DEHP + SB1 (Fig. 4d) and P_DEHP + SB2 (Fig. 4e) produced island-type features with larger pad sizes than observed for PFO and ZDDP in PFO.

3.3 Chemical Characterization of Tribofilms Using XANES

3.3.1 Phosphorus P L_{2,3}-Edge XANES

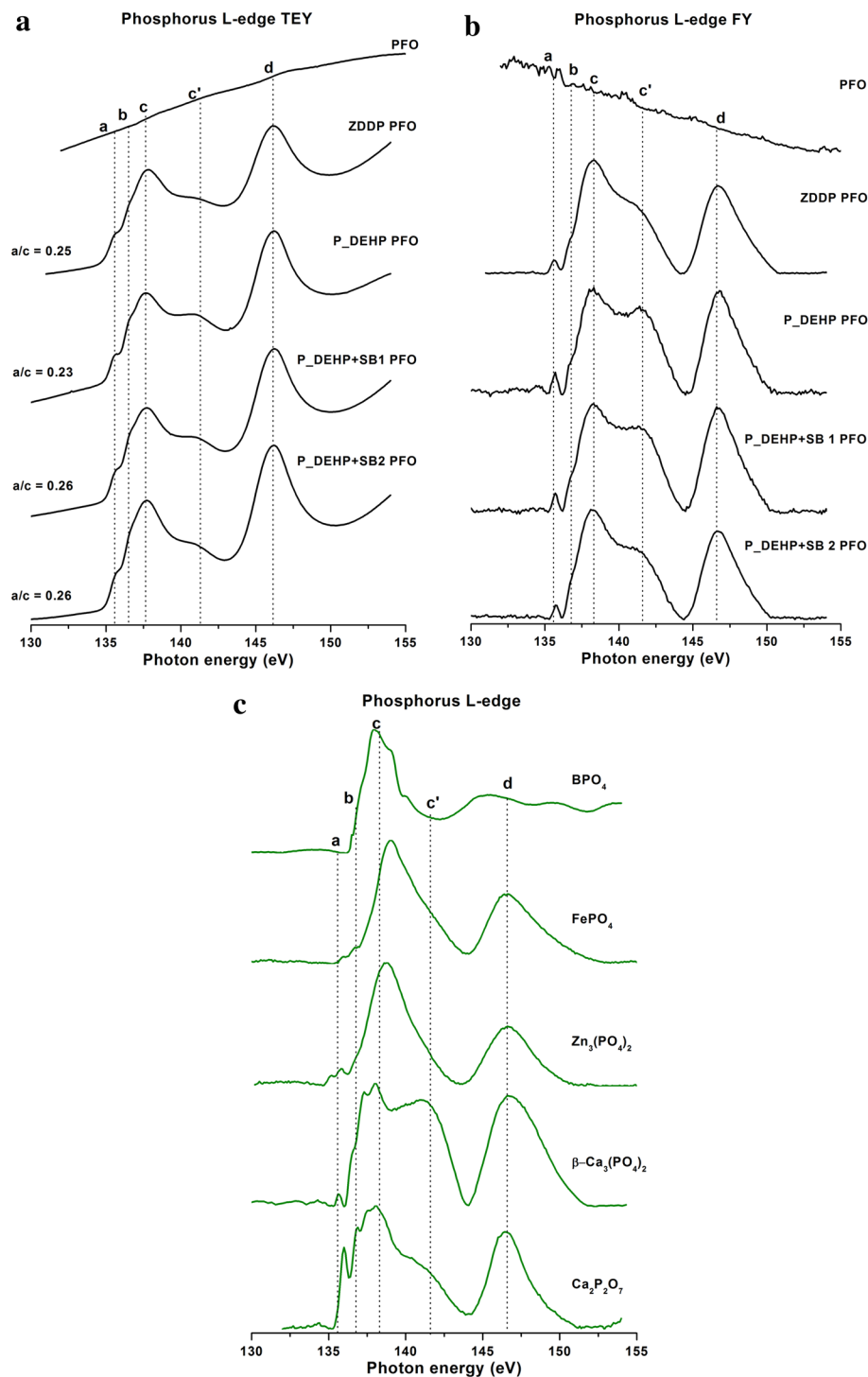
Phosphorus species in the tribofilms were determined by probing the P L-edge in both total electron yield (TEY) and fluorescent yield (FY) detection modes to obtain the local coordination of phosphorus near surface and in the bulk of tribofilms, respectively. Figure 5a, b represent the P L-edge TEY and FY spectra of the tribofilms derived from the oil blends used in this study. P L-edge spectra of model compounds are plotted in Fig. 5c for fingerprint match analysis. As expected, tribofilms from PFO did not exhibit P L-edge TEY and FY spectra since the oil did not contain phosphorus. In contrast, P L-edge TEY and FY spectra of tribofilms from oil blends with AW exhibited a main absorption edge at peak **c**, pre-edge shoulder at peaks **a** and **b**, post-edge shoulder at peak **c'** and a shape resonance at peak **d**. Comparing the spectra of tribofilms with the model compounds' spectra (Fig. 5c), peak **d** was present in all the phosphate structures while the main absorption edge peak **c** well aligned with calcium phosphates (β -Ca₃(PO₄)₂ and Ca₂P₂O₇). The main absorption edge energy for BPO₄ also closely matched with peak **c** while the main absorption edge energy for FePO₄ and Zn₃(PO₄)₂ were observed at higher photon energy than peak **c**. Furthermore, the presence of a post-edge peak **c'** in the tribofilms' spectra was found to be a characteristic peak for calcium phosphate species and is commonly observed in both β -Ca₃(PO₄)₂ and Ca₂P₂O₇. The results indicated that in tribofilms derived from oil blends containing ZDDP, P_DEHP, P_DEHP + SB1 and P_DEHP + SB2, phosphorus was primarily present in calcium phosphates, i.e., β -Ca₃(PO₄)₂ and Ca₂P₂O₇. Model compound β -Ca₃(PO₄)₂ (orthophosphate structure) exhibited higher peak intensity for peak **c'** than model compound Ca₂P₂O₇ (pyrophosphate structure). P L-edge FY spectra of P_DEHP, P_DEHP + SB1 and P_DEHP + SB2 tribofilms showed higher intensities for peak **c'** than ZDDP tribofilm. Accordingly, it is suggested that P_DEHP, P_DEHP + SB1 and P_DEHP + SB2 contributed to the formation of higher amounts of β -Ca₃(PO₄)₂.

In our previous study, the same AW chemistries were used but dissolved in a group I base oil [19]. There, ZDDP, P_DEHP, P_DEHP + SB1 and P_DEHP + SB2 exhibited the formation of zinc phosphate (in the case of ZDDP) and iron phosphate (in the case of P_DEHP, P_DEHP + SB1 and P_DEHP + SB2). Partially formulated oil used in this study contained among others detergents, hence differed

significantly from a neat base oil. Detergents, commonly used, are CaCO₃ nanoparticles that are covered with an anionic detergent, e.g., alkylbenzenesulfonate, to give a micelle structure around calcium carbonate. This explains why calcium-based detergents in the oil blends influenced the phosphorus chemistry of tribofilms formed in all cases where P was part of the AW chemistry. Sharma et al. [17, 39] also reported on the formation of calcium phosphate in tribofilms from fully formulated oils containing ZDDP and other IL structures while in base oil blends with ZDDP tribofilms were composed of zinc phosphates and IL tribofilms contained iron phosphates, respectively. In accordance, Najman et al. [36] reported that antiwear films formed from ashless AW additives incorporated calcium phosphate instead of iron phosphate when calcium-based detergents were added to the base oil blends. The standard free energy of formation ΔG^0 of the phosphate compounds, which are close to tribofilm chemistries, include -1645 kJ for FePO₄·2H₂O, -867 kJ for Zn₃(PO₄)₂·4H₂O, -3861 kJ for Ca₃(PO₄)₂ and -6669 kJ for Ca₅(PO₄)₃OH. The more negative energy of formation, the more stable the compound is. Furthermore, the enthalpy of formation ΔH^0 of -1297 kJ for FePO₄, -2891 kJ for Zn₃(PO₄)₂ and -4120 kJ for Ca₃(PO₄)₂ indicates that Fe and Zn phosphates more likely form at an earlier stage of rubbing. However, the higher stability of the Ca phosphates suggest a cation exchange in the antiwear films where Ca replaces Fe and Zn to eventually result in Ca phosphates in the tribofilm [40–42].

P L-edge TEY spectra were further analyzed for phosphate chain polymerization in the tribofilms. The phosphate chain polymerization was estimated by calculating the peak intensity ratio of peak **a** to peak **c**. Earlier studies [32, 34, 43] suggested that **a/c** ratios below 0.3 correspond to short chain phosphates and above 0.6 to long chain phosphates. The **a/c** ratios calculated from P L-edge TEY spectra are shown in Fig. 5a for all oil blends with AW additives. All AW additives used in this study formed short chain phosphates at near surface of the tribofilms (0.23–0.26). Kasrai et al. [42] reported that addition of calcium-based detergents inhibited the formation of long-chain phosphates in ZDDP tribofilms. However, we have recently discovered the formation of short chain phosphates when using AW additives in base oil blends without detergents [19]. Furthermore, Patel et al. also demonstrated that polyphosphates formed under realistic engine conditions (piston rings and cylinders in a Mack T11 engine) were short-chain phosphates of Zn. Hence, chain polymerization to give polyphosphates is less a function of the presence of Ca but rather is largely driven by the tribological conditions including contact load and lubricant availability.

Fig. 5 **a** P L-edge TEY spectra of tribofilms derived from PFO and its blends with ZDDP, P_DEHP, P_DEHP+SB1 and P_DEHP+SB2. **b** P L-edge FY spectra of tribofilms derived from PFO and its blends with ZDDP, P_DEHP, P_DEHP+SB1 and P_DEHP+SB2

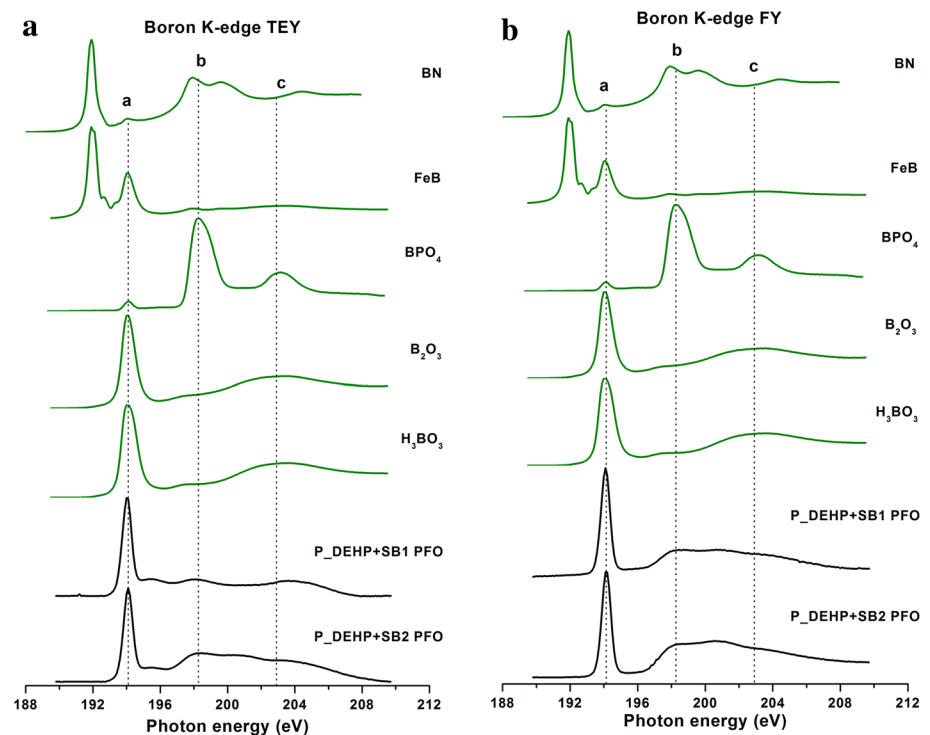


3.3.2 Boron B K-Edge XANES

The interaction of borate esters with P_DEHP in partially formulated oil blends was examined by probing B K-edge spectra of tribofilms. B K-edge TEY and FY spectra of tribofilms formed from P_DEHP+SB1 and P_DEHP+SB2 (plotted in black line) are shown in Fig. 6a, b and compared with model compounds (plotted in green lines). B

K-edge TEY probes the tribofilm surface (~6 nm) and FY provides information about the tribofilm bulk (~100 nm) [44]. Different boron species can be distinguished by examining their characteristic absorption edge (discussed in [19]). In Fig. 6a, b, three peaks were assigned to peak **a**, peak **b** and peak **c**. Peak **a** and peak **c** appeared at photon energies of 194.0 eV and 202.9 eV, respectively, that were attributed to trigonal coordination of boron species [44].

Fig. 6 **a** B K-edge TEY spectra of tribofilms derived from P_DEHP + SB1 and P_DEHP + SB2 in PFO (plotted in black lines) and compared with model compounds (plotted in green lines). **b** B K-edge FY spectra of tribofilms derived from P_DEHP + SB1 and P_DEHP + SB2 in PFO (plotted in black lines) and compared with model compounds (plotted in green lines)

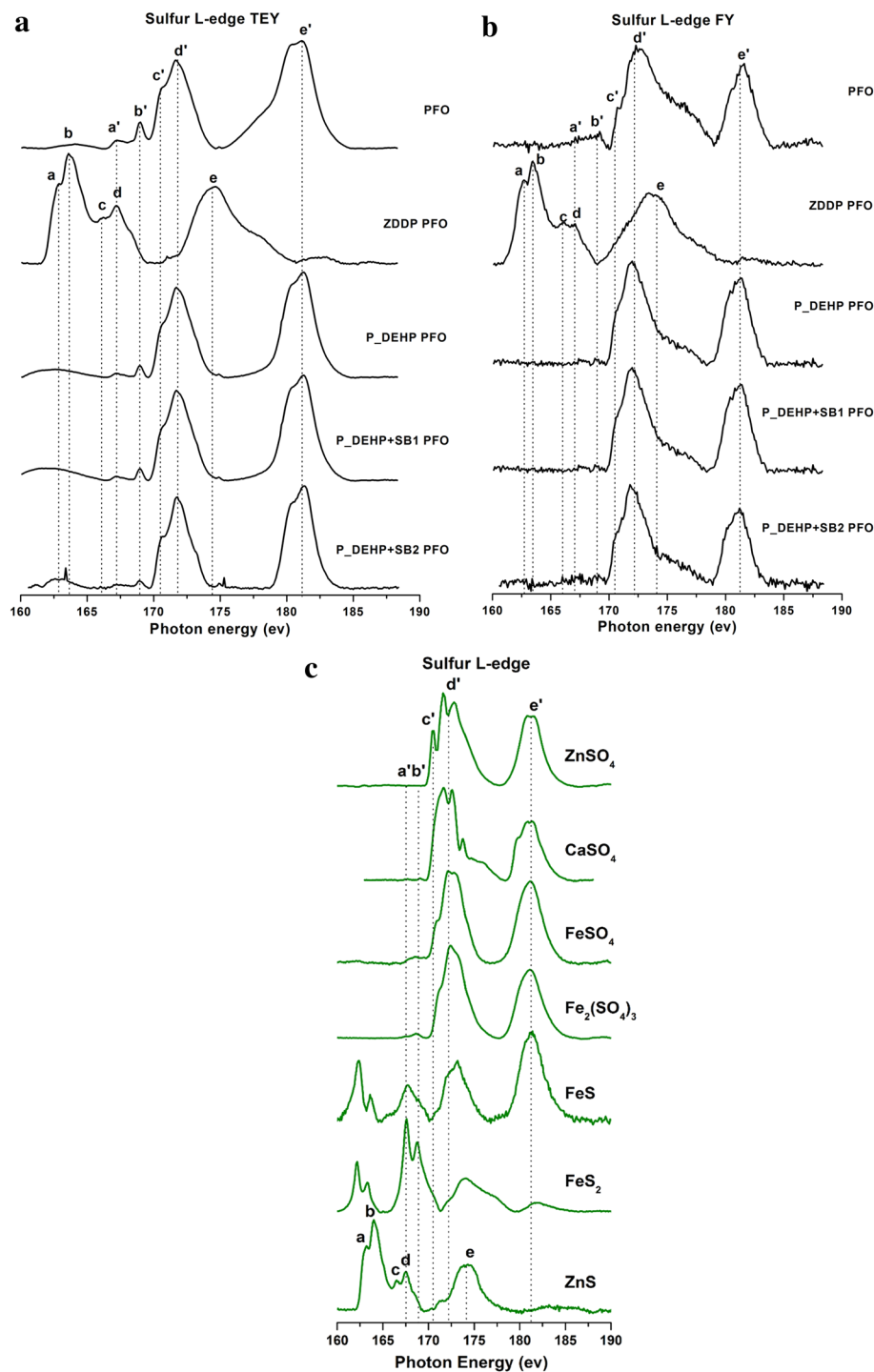


Peak **b** occurred at a photon energy of 198.4 eV that corresponded to tetrahedral coordination [44]. Peaks **a** and **c** were commonly present in B_2O_3 and H_3BO_3 . BPO_4 exhibited peak **a**, **b** and **c** where peak **c** was slightly shifted to higher photon energy. Peak **b** from tetrahedral B was the dominant peak, since the compound in its pure form has boron in tetrahedral coordination. Relatively weak peaks **a** and **c** in BPO_4 spectra possibly originated from surface modification [44]. The B K-edge TEY and FY spectra of the tribofilms exhibited a strong absorption edge at peak **a** but little intensities of peak **b** and **c** which was slightly shifted to higher photon energy (204 eV). B K-edge TEY spectra revealed that boron at near surface (TEY) and in the bulk (FY) of the tribofilms was dominantly present as trigonal boron (B_2O_3/H_3BO_3). In addition to that, presence of weak peaks **a** and **c** suggested two possibilities: first, the likelihood for the formation of BPO_4 in the tribofilms due to the interaction of borate esters and P_DEHP and second, a partially thermo-mechanical transformation of boron from trigonal to tetrahedral coordination in the tribofilms induced by shearing [45]. In the base oil study (discussed in [19]), synergism between borate esters and P_DEHP has shown a clear absorption edge at 198.4 eV which could be attributed to the formation of BPO_4 . In this study, it can be speculated that a preferential formation of calcium phosphates occurred due to interaction between calcium and phosphorus species that essentially inhibited the formation of both $FePO_4$ and BPO_4 , which were evident in tribofilms formed in base oil blends.

3.3.3 Sulfur S L-Edge XANES

The primary source of sulfur in the tribofilms was the detergent made up of overbased calcium sulfonate. In addition, ZDDP also contained sulfur in its original structure. Sulfur species formed in the tribofilms using oil blends from PFO with or without AW additives were probed by acquiring the S L-edge spectra. The S L-edge spectra were acquired in both TEY and FY mode to examine the sulfur chemistries in the tribofilms as a function of film thickness [23]. S L-edge spectra of the tribofilms are presented in Fig. 7a, b and compared with model compound spectra in Fig. 7c. Differences in the spectra of the model compounds and their relative peak energies are detailed by Kim et al. [30]. S L-edge TEY and FY spectra of the tribofilms exhibited similar absorption signatures for each oil blend, but the signal to noise ratio was reduced in FY spectra. No significant changes were observed in the sulfur chemistries from the near-surface region towards the bulk of the individual tribofilms besides the observation that overall sulfur contents were higher in the near-surface region than in the bulk. But different sulfur species were found in the tribofilms formed from PFO and its oil blends with AW additives. By fingerprint match analysis of the tribofilms from P_DEHP, P_DEHP + SB1 and P_DEHP + SB2 each in PFO with the model compounds, peaks in the S L-edge spectra labeled as peak **a'**, **b'**, **c'**, **d'** and **e'** could be assigned as follows: peak **a'** and **b'** referred to sulfide (-2 oxidation state) species primarily in iron sulfides.

Fig. 7 **a** S L-edge TEY spectra of tribofilms derived from PFO and its blends with ZDDP, P_DEHP, P_DEHP+SB1 and P_DEHP+SB2. **b** S L-edge FY spectra of tribofilms derived from PFO and its blends with ZDDP, P_DEHP, P_DEHP+SB1 and P_DEHP+SB2. **c** S L-edge FY spectra of model compounds



Peak **e'** was commonly present in all the sulfate structures which confirmed that sulfur was also present in sulfates (+6 oxidation state). In addition, presence of peaks **c'** and **d'** suggested that the sulfates were mainly bound in iron sulfate since peak **c'** represented the pre-edge shoulder of the iron sulfate absorption edge denoted as peak **d'**. Since Zn was not present in these tribofilms, we eliminated the

possibility of ZnSO₄ whereas we could not completely exclude the probability of the formation of CaSO₄. In the case of tribofilms from ZDDP in PFO, peaks **a**, **b**, **c**, **d** and **e** aligned well with the ZnS spectra. Thus, tribofilms from oil blends with ZDDP contained sulfur primarily in the form of the sulfide (-2 oxidation state).

3.3.4 Calcium Ca K-Edge XANES

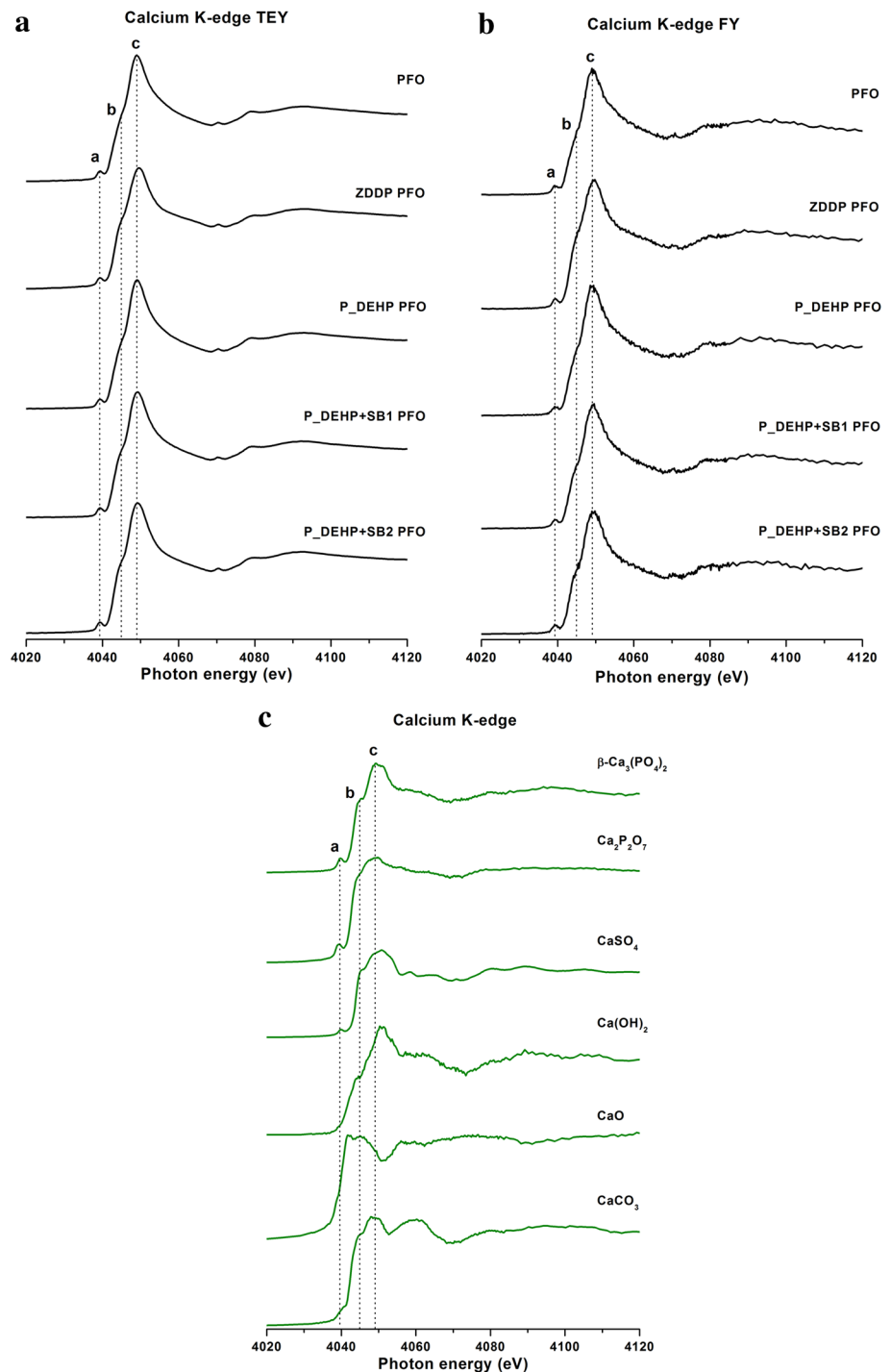
Calcium K-edge spectra were also acquired to complement the results observed from P L-edge and S L-edges. Ca K-edge TEY and FY spectra of the tribofilms are plotted in Fig. 8a, b and compared with model compounds in Fig. 8c. Three peaks were identified and labeled as peak **a**, **b** and **c**. By fingerprint matching with model compounds, the

presence of either or both calcium phosphate and calcium sulfate was determined.

3.3.5 Discussion of XANES Findings

A detailed understanding of the mechanism of tribofilm formation using P_DEHP and binary mixtures of P_DEHP and borate esters SB1 and SB2 as AW additives could be

Fig. 8 **a** Ca K-edge TEY spectra of tribofilms derived from PFO and its blends with ZDDP, P_DEHP, P_DEHP+SB1 and P_DEHP+SB2. **b** Ca K-edge FY spectra of tribofilms derived from PFO and its blends with ZDDP, P_DEHP, P_DEHP+SB1 and P_DEHP+SB2. **c** Ca K-edge FY spectra of model compounds



developed. P L-edge spectra indicated that phosphorus was mainly incorporated as calcium phosphates in the antiwear films. The interaction of the calcium cation from the overbased detergent with the phosphorus-containing AW additives ZDDP and P_DEHP offered the formation of stable films in terms of free energy and enthalpy of formation, which were preferred over phosphates with iron or zinc. B K-edge spectra suggested that the addition of borate esters to P_DEHP resulted in B_2O_3/H_3BO_3 tribofilms enhanced by BPO_4 . However, calcium phosphate formation was found to be dominant during rubbing rather than the formation of boron phosphate. As to sulfur, the kind of sulfur species that contributed to the tribofilms was significantly dependent on the sulfur chemistries available in the oil blends. For oils with ZDDP, sulfur was largely present as zinc sulfide. Oil blends with sulfonate detergent as major sulfur source, i.e., PFO when used alone, P_DEHP, P_DEHP + SB1 and P_DEHP + SB2 each in PFO, resulted in the formation of mainly iron sulfates on the rubbed surfaces. Ca K-edge spectra confirmed the formation of calcium phosphates on the surfaces and hence complemented the findings from P L-edge spectra.

4 Conclusions

The friction and wear behavior of fully formulated engine oils with a phosphonium phosphate ionic liquid (P_DEHP) and two borate esters (SB1 and SB2) were benchmarked against oil blends without AW additives and with ZDDP. Friction with ZDDP stabilized at ~ 0.14 whereas friction was found at ~ 0.12 with all other oil blends. Results from tribological experiments revealed significant improvement in wear protection (50% and more) with P_DEHP and the binary additive mixtures P_DEHP + SB1 and P_DEHP + SB2 compared to the oil without AW additives and the oil with ZDDP.

Tribofilms characterization by XANES indicated that phosphorus was primarily present in the form of calcium phosphates whenever phosphorus-based AW additives were used. ZDDP resulted in the incorporation of sulfur primarily in the form of zinc sulfides in the tribofilms. Partially formulated oil (without AW additives) and oils with P_DEHP and mixtures of P_DEHP + SB1 and P_DEHP + SB2 formed tribofilms that contained iron sulfates and iron sulfides and to some extent calcium sulfates. Boron was primarily present in the form of boric acid/boron oxide as well as boron phosphate to a smaller extent. In summary, it can be said the interplay of P_DEHP and SB resulted in tribofilms composed calcium phosphates, calcium sulfates, iron sulfates, iron sulfides and boron oxide/boric acid enhanced by boron phosphate.

The formation of calcium phosphates could be observed, which are chemically more stable than iron and zinc phosphates detected in tribofilms from AW additives in base oils as recently reported. The findings in this study also demonstrate the importance of the use of oil blends that represent fully formulated oils to account for the interactions of AW additives with other compounds, in particular overbased detergents in the case of engine oils.

Acknowledgements XANES experiments were conducted at the Canadian Light Source, Saskatoon, Saskatchewan, Canada that is supported by NSERC, NRC, CIHR and the University of Saskatchewan. Tribological tests were performed at Argonne National Laboratory and were supported by the U.S. Department of Energy, Office of Energy Efficiency and Renewable Energy, Office of Vehicle Technology under contract DE-AC02-06CH11357. Scanning probe microscopy experiments were conducted at Center for Characterization for Materials and Biology at The University of Texas at Arlington. This work was also supported by the "Austrian COMET-Program" in the frame of K2 XTribology (Project No. 849109).

References

- Sharma, V., Doerr, N., Aswath, P.: Chemical-mechanical properties of tribofilms and its relation to ionic liquid chemistry. *RSC Adv.* **6**, 22341–22356 (2016)
- Somers, A.E., Khemchandani, B., Howlett, P.C., Sun, J., MacFarlane, D.R., Forsyth, M.: Ionic liquids as antiwear additives in base oils: influence of structure on miscibility and antiwear performance for steel on aluminum. *ACS Appl. Mater. Interfaces* **5**, 11544–11553 (2013)
- Anand, M., Hadfield, M., Viesca, J., Thomas, B., Battez, A.H., Austen, S.: Ionic liquids as tribological performance improving additive for in-service and used fully-formulated diesel engine lubricants. *Wear* **334**, 67–74 (2015)
- Barnhill, W.C., Qu, J., Luo, H., Meyer, H.M., Ma, C., Chi, M., et al.: Phosphonium-organophosphate ionic liquids as lubricant additives: effects of cation structure on physicochemical and tribological characteristics. *ACS Appl. Mater. Interfaces* **6**, 22585–22593 (2014)
- Pisarova, L., Gabler, C., Dörr, N., Pittenauer, E., Allmaier, G.: Thermo-oxidative stability and corrosion properties of ammonium based ionic liquids. *Tribol. Int.* **46**, 73–83 (2012)
- Cai, M., Liang, Y., Yao, M., Xia, Y., Zhou, F., Liu, W.: Imidazolium ionic liquids as antiwear and antioxidant additive in poly (ethylene glycol) for steel/steel contacts. *ACS Appl. Mater. Interfaces* **2**, 870–876 (2010)
- Minami, I.: Ionic liquids in tribology. *Molecules* **14**, 2286–2305 (2009)
- Yu, B., Bansal, D.G., Qu, J., Sun, X., Luo, H., Dai, S., et al.: Oil-miscible and non-corrosive phosphonium-based ionic liquids as candidate lubricant additives. *Wear* **289**, 58–64 (2012)
- Gusain, R., Gupta, P., Saran, S., Khatri, O.P.: Halogen-free bis (imidazolium)/bis (ammonium)-di [bis (salicylato) borate] ionic liquids as energy efficient and environment-friendly lubricant additives. *ACS Appl. Mater. Interfaces* **6**(17), 15318–15328 (2014)
- Qu, J., Luo, H., Chi, M., Ma, C., Blau, P.J., Dai, S., et al.: Comparison of an oil-miscible ionic liquid and ZDDP as a lubricant anti-wear additive. *Tribol. Int.* **71**, 88–97 (2014)
- Totolin, V., Minami, I., Gabler, C., Brenner, J., Dörr, N.: Lubrication mechanism of phosphonium phosphate ionic liquid additive

- in alkylborane–imidazole complexes. *Tribol. Lett.* **53**, 421–432 (2014)
12. Qu, J., Blau, P.J., Dai, S., Luo, H., Meyer, H.M.: Ionic liquids as novel lubricants and additives for diesel engine applications. *Tribol. Lett.* **35**, 181–189 (2009)
 13. Jiménez, A.E., Bermúdez, M.: Ionic liquids as lubricants of titanium–steel contact. *Tribol. Lett.* **33**, 111–126 (2009)
 14. Jimenez, A., Bermudez, M.: Ionic liquids as lubricants of titanium–steel contact. Part 2: friction, wear and surface interactions at high temperature. *Tribol. Lett.* **37**, 431–443 (2010)
 15. Kronberger, M., Pejaković, V., Gabler, C., Kalin, M.: (2012) How anion and cation species influence the tribology of a green lubricant based on ionic liquids. *Proc. Inst. Mech. Eng. Part J.* **226**, 933–951
 16. Bermúdez, M., Jiménez, A., Sanes, J., Carrión, F.: Ionic liquids as advanced lubricant fluids. *Molecules* **14**, 2888–2908 (2009)
 17. Sharma, V., Gabler, C., Doerr, N., Aswath, P.B.: Mechanism of tribofilm formation with P and S containing ionic liquids. *Tribol. Int.* **92**, 353–364 (2015)
 18. González, R., Bartolomé, M., Blanco, D., Viesca, J., Fernández-González, A., Battez, A.H.: Effectiveness of phosphonium cation-based ionic liquids as lubricant additive. *Tribol. Int.* **98**, 82–93 (2016)
 19. Sharma, V., Doerr, N., Erdemir, A., Aswath, P.: Interaction of phosphonium ionic liquids with borate esters at tribological interfaces. *RSC Adv.* **6**, 53148–53161 (2016)
 20. Qu, J., Bansal, D.G., Yu, B., Howe, J.Y., Luo, H., Dai, S., et al.: Antiwear performance and mechanism of an oil-miscible ionic liquid as a lubricant additive. *ACS Appl. Mater. Interfaces* **4**, 997–1002 (2012)
 21. Grocholski, B.: Additive explanation for anti-wear. *Science.* **348**, 87–88 (2015)
 22. Qu, J., Barnhill, W.C., Luo, H., Meyer, H.M., Leonard, D.N., Landauer, A.K., et al.: Synergistic effects between phosphonium-alkylphosphate ionic liquids and zinc dialkyldithiophosphate (ZDDP) as lubricant additives. *Adv. Mater.* **27**, 4767–4774 (2015)
 23. Kasrai, M., Lennard, W.N., Brunner, R.W., Bancroft, G.M., Bardwell, J.A., Tan, K.H.: Sampling depth of total electron and fluorescence measurements in Si L- and K-edge absorption spectroscopy. *Appl. Surf. Sci.* **99**, 303–312 (1996)
 24. Parekh, K., Chen, X., Aswath, P.B.: Synthesis of fluorinated ZDDP compounds. *Tribol. Lett.* **34**, 141–153 (2009)
 25. Sharma, V., Erdemir, A., Aswath, P.B.: An analytical study of tribofilms generated by the interaction of ashless antiwear additives with ZDDP using XANES and nano-indentation. *Tribol. Int.* **82**, 43–57 (2015)
 26. Sharma, V., Uy, D., Gangopadhyay, A., O'Neill, A., Paxton, W.A., Sammut, A., et al.: Structure and chemistry of crankcase and exhaust soot extracted from diesel engines. *Carbon.* **103**, 327–338 (2016)
 27. Chen, X., Elsenbaumer, R.L., Aswath, P.B.: Synthesis and tribological behavior of ashless alkylphosphorofluorodithioates. *Tribol. Int.* **69**, 114–124 (2013)
 28. Chen, X., Kim, B., Elsenbaumer, R., Aswath, P.B.: Synthesis and antiwear behavior of alkylthioperoxydiphosphates. *Tribology* **6**(3), 121–133 (2012)
 29. Nicholls, M., Najman, M.N., Zhang, Z., Kasrai, M., Norton, P.R., Gilbert, P.U.P.A.: The contribution of XANES spectroscopy to tribology. *Can. J. Chem.* **85**, 816–830 (2007)
 30. Kim, B., Mourhatch, R., Aswath, P.B.: Properties of tribofilms formed with ashless dithiophosphate and zinc dialkyl dithiophosphate under extreme pressure conditions. *Wear.* **268**, 579–591 (2010)
 31. Li, Y., Pereira, G., Lachenwitzer, A., Kasrai, M., Norton, P.R.: X-ray absorption spectroscopy and morphology study on antiwear films derived from ZDDP under different sliding frequencies. *Tribol. Lett.* **27**, 245–253 (2007)
 32. Li, Y., Pereira, G., Kasrai, M., Norton, P.R.: Studies on ZDDP anti-wear films formed under different conditions by XANES spectroscopy, atomic force microscopy and ³¹P NMR. *Tribol. Lett.* **28**, 319–328 (2007)
 33. Nicholls, M.A., Do, T., Bancroft, G.M., Norton, P.R., Kasrai, M., Capehart, T.W., et al.: Chemical and mechanical properties of ZDDP antiwear films on steel and thermal spray coatings studied by XANES spectroscopy and nanoindentation techniques. *Tribol. Lett.* **15**(3), 241–248 (2003)
 34. Najman, M.N., Kasrai, M., Bancroft, G.M., Frazer, B.H., DeStatio, G.: The correlation of microchemical properties to antiwear (AW) performance in ashless thiophosphate oil additives. *Tribol. Lett.* **17**(4), 811–822 (2004)
 35. Najman, M.N., Kasrai, M., Bancroft, G.M.: Chemistry of antiwear films from ashless thiophosphate oil additives. *Tribol. Lett.* **17**(2), 217–229 (2004)
 36. Najman, M., Kasrai, M., Michael Bancroft, G., Davidson, R.: Combination of ashless antiwear additives with metallic detergents: Interactions with neutral and overbased calcium sulfonates. *Tribol. Int.* **39**, 342–355 (2006)
 37. Pereira, G., Munoz-Paniagua, D., Lachenwitzer, A., Kasrai, M., Norton, P.R., Capehart, T.W., et al.: A variable temperature mechanical analysis of ZDDP-derived antiwear films formed on 52100 steel. *Wear* **262**, 461–470 (2007)
 38. Warren, O.L., Graham, J.F., Norton, P.R., Houston, J.E., Michalske, T.A.: Nanomechanical properties of films derived from zinc dialkyldithiophosphate. *Tribol. Lett.* **4**, 189–198 (1998)
 39. Aswath, P., Chen, X., Sharma, V., Igartua, M.A., Pagano, F., Binder, W., et al.: (2013) Synergistic mixtures of ionic liquids with other ionic liquids and/or with ashless thiophosphates for antiwear and/or friction reduction applications. U.S. Patent Application No. 13/889,037
 40. Willermet, P.A., Dailey, D.P., Carter, R.O., Schmitz, P.J., Zhu, W., Bell, J.C., et al.: The composition of lubricant-derived surface layers formed in a lubricated cam/tappet contact, II. Effects of adding overbased detergent and dispersant to a simple ZDTP solution. *Tribol. Int.* **28**(3), 163–175 (1995)
 41. Wan, Y., Suominen Fuller, M.L., Kasrai, M., Bancroft, G.M., Fyfe, K., Torkelson, J.R., et al.: Effects of detergent on the chemistry of tribofilms from ZDDP: studied by X-ray absorption spectroscopy and XPS. In: Dowson, D., Priest, M., Dalmaz, G., Lubrecht, A.A. (eds.) *Tribology Series*, vol. 40, pp. 155–166. Elsevier, Amsterdam (2002)
 42. Kasrai, M., Fuller, M.S., Bancroft, G.M., Ryason, P.R.: X-ray absorption study of the effect of calcium sulfonate on antiwear film formation generated from neutral and basic ZDDPs: part 1—phosphorus species. *Tribol. Trans.* **46**, 534–542 (2003)
 43. Yin, Z., Kasrai, M., Bancroft, G.M., Tan, K.H., Feng, X.: X-ray-absorption spectroscopic studies of sodium polyphosphate glasses. *Phys. Rev. B* **51**, 742–750 (1995)
 44. Kasrai, M., Fleet, M.E., Muthupari, S., Li, D., Bancroft, G.: Surface modification study of borate materials from B K-edge X-ray absorption spectroscopy. *Phys. Chem. Miner.* **25**, 268–272 (1998)
 45. Zhang, Z., Yamaguchi, E.S., Kasrai, M., Bancroft, G.M.: Interaction of ZDDP with borated dispersant using XANES and XPS. *Tribol. Trans.* **47**, 527–536 (2004)

Publisher's Note Springer Nature remains neutral with regard to jurisdictional claims in published maps and institutional affiliations.